Engineering xxx (xxxx) xxx

Contents lists available at ScienceDirect

Engineering

journal homepage: www.elsevier.com/locate/eng

Research
Agricultural Engineering—Article

Nanobubbles for the Mitigation of Fouling in Wastewater Distribution Systems

Yang Xiao [a,b], Bo Zhou [a,b], Siyuan Tan [a], Lei Li [c], Tahir Muhammad [a], Buchun Si [a], Changjian Ma [d], Sunny C. Jiang [e,*], Yunkai Li [a,b,*]

[a] College of Water Resources and Civil Engineering, China Agricultural University, Beijing 100083, China
[b] Engineering Research Center for Agricultural Water-Saving and Water Resources (Ministry of Education of the People's Republic of China), China Agricultural University, Beijing 100083, China
[c] School of Environment and Civil Engineering, Dongguan University of Technology, Dongguan 523808, China
[d] State Key Laboratory of Nutrient Use and Management, Institute of Agricultural Resources and Environment, Shandong Academy of Agricultural Sciences, Jinan 250100, China
[e] Department of Civil and Environmental Engineering, University of California-Irvine, Irvine, CA 92617, USA

ARTICLE INFO

Article history:
Available online xxxx

Keywords:
Biofouling
Scaling
Colloidal fouling
Wastewater
Antifouling mechanism

ABSTRACT

The increasing demand for wastewater treatment has become a notable trend for addressing global water scarcity. However, fouling is a significant challenge for wastewater distribution engineering systems. This study provides an approach using nanobubbles (NBs) to control fouling. The antifouling capacities of three types of NBs, six oxygen concentrations, and two application procedures (prevention and removal) are investigated. The results show that NBs effectively mitigate composite fouling—including biofouling, inorganic scaling, and particulate fouling—in comparison with the no-NBs group. More specifically, hydroxyl radicals generated by the self-collapse of NBs oxidize organics and kill microorganisms in wastewater. The negatively charged surfaces of the NBs transform the crystalline form of $CaCO_3$ from calcite to looser aragonite, which reduces the likelihood of ion precipitation. Furthermore, the NBs gas-liquid interfaces act as gas "bridges" between colloidal particles, enhancing the removal of particles from wastewater. Lastly, although the NBs inhibit the growth of fouling, they do not significantly remove the already adhered fouling in no-NBs treated groups. This study anticipates that the application of NBs will address the significant fouling issue for various wastewater distribution engineering systems in order to meet the global challenge of sustainable water supplies.

1. Introduction

Climate change and population growth continue to intensify global water scarcity [1], necessitating an increased reliance on partially treated wastewater to meet agricultural, industrial, and municipal water demands [2–4]. However, fouling—that is, the deposition of undesirable matter on surfaces [5–8]—is the cause of various technical and economic issues in wastewater treatment and distribution systems [9,10]. The increase in fouling-related costs has been estimated to be approximately 0.25% of the global gross domestic product [11]. Thus, fouling has emerged as a critical challenge for wastewater distribution systems.

Fouling is generally classified into several categories: biofouling, particulate or colloidal fouling, inorganic or precipitate fouling, and organic fouling [12]. As wastewater always contains an active quantity of microorganisms, along with dissolved salts, suspended particles, and organics, various kinds of fouling often occur simultaneously, resulting in composite fouling. At present, chemical dosing is the main method of fouling control [13]. However, the use of chemicals must be kept to a minimum because residual chemicals can pose long-term environmental and human health risks [14,15]. Moreover, chemical methods are ineffective for mitigating composite fouling in wastewater distribution systems [13,16]. For example, chlorination effectively controls biofouling by killing bacteria but does not prevent scaling and particulate fouling [17]. Therefore, simply inactivating bacteria does little to alleviate fouling. As a result, effective fouling control requires the management of composite fouling (i.e., biofilms, precipitates, and colloidal

* Corresponding authors.
E-mail addresses: sjiang@uci.edu (S.C. Jiang), yunkai@cau.edu.cn (Y. Li).

https://doi.org/10.1016/j.eng.2023.10.013
2095-8099/

particulates). Such management is especially important because almost all fouling in wastewater distribution systems can be categorized as composite fouling.

Nanobubbles (NBs), which are defined as gas bubbles in water with diameters <1 μm [18], offer a new approach for fouling control with minimal environmental impacts [19]. In comparison with conventional bubbles, NBs have longer periods of stability, higher specific surface areas (SSAs), lower buoyancy, and superior adsorption capacities [20]. NBs have attracted a great deal of attention for various applications, including biological aeration, water oxidation, disinfection, particle flotation, and agriculture irrigation [18]. They have been shown to delay membrane fouling [21], remove organic fouling [22], and reduce bacterial biofilms in irrigation pipes [3]; however, each of these studies has targeted a single type of fouling. Although these results are promising, the effectiveness of NBs in mitigating composite fouling has not been demonstrated. Composite fouling mitigation is expected to be more challenging than the management of a single type of fouling because fouling becomes increasingly difficult to control when there are strong interactions among various types of foulants. For example, biofouling can accelerate the growth of inorganic fouling [23], and composite fouling layers have greater mechanical strength than those formed due to a single type of fouling [24].

Another factor limiting the practical application of NBs is that the outcomes reported in the literature are inconsistent or contradictory, as NBs antifouling mechanisms are still unclear. Some researchers have suggested that the physical properties of NBs play important roles in fouling control. For example, early studies reported that the shear forces of NBs acted either directly to remove foulants [22,25–27] or through the destruction of concentration polarization on membrane surfaces to prevent scaling [28]. In contrast, Xiao et al. [3] reported that NBs did not remove pre-existing fouling. Furthermore, some studies have indicated that the gases in NBs—particularly oxygen—are important for fouling control. The breakdown of oxygen molecules is key in the formation from NBs of hydroxyl radicals (·OH) [29], which are linked to water sterilization and organic oxidation. For example, pure oxygen NBs have been reported to be more useful for killing *Vibrio parahaemolyticus* than air NBs [30]. To date, the role of NBs internal gases in fouling control remains unknown. Overall, the antifouling mechanisms of NBs—particularly for various types of fouling mitigation—are not fully understood.

The current study reports on a reduction in composite fouling on the surfaces of a wastewater distribution pipe that recycles wastewater for agricultural irrigation. The antifouling capacities of NBs produced using two types of inert gases and pure oxygen were compared in order to isolate the role of oxygen gas and compare its relative importance with the role of NBs physical properties during fouling control. The effects of oxygen NBs antifouling at concentrations ranging from 5% to 100% were evaluated. This study also assessed the ability of NBs to prevent the onset of fouling and to remove pre-existing fouling layers. The objectives of this study were to ① determine the specific mechanisms for biofouling, scaling, and particulate fouling reduction by means of NBs; and ② provide useful practices for the successful application of NBs in wastewater distribution engineering systems.

2. Materials and methods

2.1. Experimental setup and treatments

NBs antifouling effectiveness was evaluated in an agricultural wastewater distribution system (Fig. 1) that was typically plagued with composite fouling. NBs are commonly used in agricultural irrigation to promote seed germination and plant growth [31]. The experimental water was a mixture of treated swine wastewater, referred to as "biogas slurry," and groundwater at a ratio of 1:8. The biogas slurry, groundwater, and mixed water were stored in three tanks at the inlet of the experimental platform. The biogas slurry was sequentially prefiltered through 0.85-mm and 0.42-mm pore-size screen filters to reduce particulate matter before being mixed with groundwater. After mixing, the stream was filtered through 0.1-mm pore-size disc filters. The filtered experimental water quality is shown in Table S1 in Appendix A.

The treated wastewater was fed into an NBs generator (XZCP-K-1.5; Xiazhichun, China) for about 4 h to create saturated NBs-infused water, where the NBs concentration of the NB-saturated water was defined as 100%. The NBs lifetime (i.e., the time required for the NB-infused water to revert back to normal water) was about 400 h. Pure oxygen (O_2) and two inert gases (nitrogen (N_2) and helium (He)) were used for NBs generation. The NBs selection considered two factors. First, since the inert gas NBs did not perform the functions of oxygen gas, these experiments served to isolate the role of oxygen gas and compare it with the roles of NBs' physical properties during fouling control. Second, the selection of NBs types considered NBs application in agricultural irrigation. O_2 is the most commonly used NBs source in agricultural irrigation, where it is used to increase soil oxygen content and improve crop quality and yield [32,33]. In comparison, N_2 NBs can increase NH_4^+ release from soil and the proliferation of nitrogen-fixing bacteria [31]. The bubble size and density distributions for different types of NBs at saturated gas concentrations are shown in Fig. S1 in Appendix A. NBs properties were also characterized by size, specific surface area (SSA), and specific surface pressure (ΔP). Detailed information is provided in Section S1 in Appendix A. In addition to experiments with saturated NBs, water infused with 5%, 25%, 50%, and 75% saturated oxygen NBs was created by mixing saturated NBs water with water containing no NBs.

The NB-infused water was pumped into the inlets of the experimental platform, which resembled an irrigation water delivery system (Fig. 1). The test platform was made up of six layers of pipelines, with eight identical 1-m long pipes for replication in each layer. The water flow rate in the pipe was 0.2 $m \cdot s^{-1}$, which is comparable with the hydraulic conditions in agricultural irrigation pipelines [34]. Based on the working life of the irrigation system, the system was run for 10 h per day for a total of 900 h [3]. Two types of NBs antifouling strategies were investigated: One strategy examined continuous NBs application for fouling prevention, while the other tested pre-existing foulant removal by means of NBs. The foulant-removal experiments were run for 24 h in pre-fouled pipes. To assess fouling mitigation by NBs treatments, the pipes were retrieved at 300, 600, and 900 h (representing the early, middle, and end of the operation life of the irrigation system) after the initiation of the experiments. As shown in Table 1, treatment groups were investigated according to NBs gas type, concentration, and application strategy.

2.2. Water quality testing

To understand the water quality changes induced by the NBs, the water pH, electrical conductivity (EC), oxidation–reduction potential (ORP), surface tension (ST), chemical oxygen demand (COD), biochemical oxygen demand (BOD), zeta potential (ZP), aerobic heterotrophic plate count (AHPC), and hydroxyl radicals were measured for each experimental group. Detailed information is provided in Section S2 in Appendix A.

2.3. Total fouling content and morphology

The total fouling content was assessed according to the dry weight of the foulants collected from the water distribution pipes,

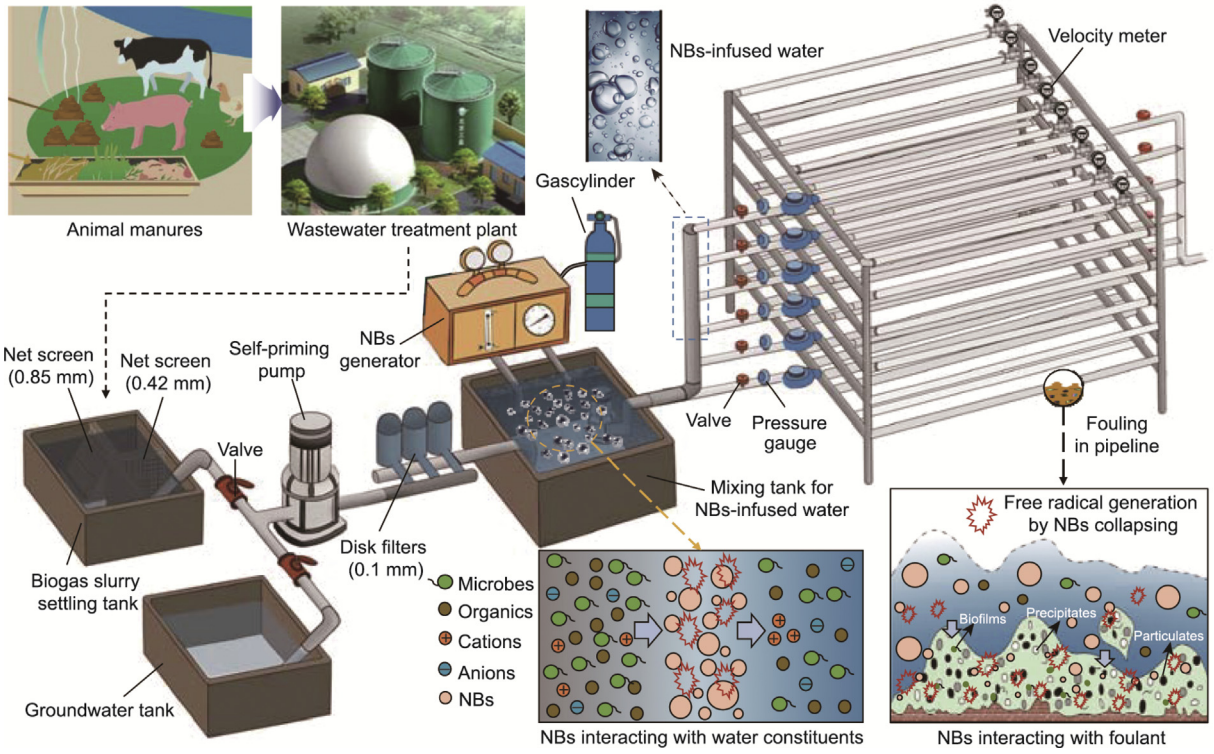

Fig. 1. Experimental setup for investigating the effect of NBs on fouling mitigation. The control treatment (not shown) consists of an identical setup without an NBs generator.

Table 1
Concentrations and types of NBs used in experimental treatments for fouling control.

Application mode	Proportion of saturated NBs water	Gas in NBs	Treatment group
Negative control (CK)	0%	None	CK
Prevention strategy	5%	Oxygen	O_2_5%
	25%	Oxygen	O_2_25%
	50%	Oxygen	O_2_50%
	75%	Oxygen	O_2_75%
	100%	Oxygen	O_2_100%
	100%	Nitrogen	N_2_100%
	100%	Helium	He_100%
Removal strategy	5%	Oxygen	O_2_5%_RM
	25%	Oxygen	O_2_25%_RM
	50%	Oxygen	O_2_50%_RM
	75%	Oxygen	O_2_75%_RM
	100%	Oxygen	O_2_100%_RM
	100%	Nitrogen	N_2_100%_RM
	100%	Helium	He_100% _RM

Saturated NB-infused water has a concentration of 100%, other concentrations NB-infused water was produced by mixing NBs saturated water and non-NBs water. In the prevention strategy, NBs were continuously added to wastewater for 900 h. In the removal strategy, NB-infused water with different types and concentrations were applied for 24 h to remove pre-formed fouling in pipes at three different timepoints (300, 600, and 900 h).

as previously described in Ref. [13]. In brief, three identical pipes were extracted from the experimental platform at 300, 600, and 900 h after the onset of the experimental trial. The weights of the pipes with the foulant attached and after foulant removal were determined by weighing the dried pipes. The difference between the two weights (i.e., with and without foulant) was taken as the weight of the foulant. In addition, one pipe with attached foulant was cut open, freeze-dried (Freezer Dryer 9511; Kenta, China), sputter-coated with gold, and examined using scanning electron microscopy (SEM; SU3500; Hitachi, Japan) for morphological observations.

2.4. Biofouling assessment

Quantitative real-time polymerase chain reaction (qPCR) (ABI; GeneAmp 9700, USA) for the 16S rRNA gene was used to determine the total microbial quantity (represented by the copy numbers per unit mass) for the fresh foulant collected from the pipe surfaces. Extracellular polymeric substance (EPS) measurements were carried out using the phenol-sulfuric acid technique [35] and the Lowry method [36] for polysaccharides and proteins, respectively.

DNeasy PowerSoil Pro Kits (QIAGEN, USA) were used to extract microbial DNA from fresh foulants. A spectrophotometer (NanoDrop2000; Thermo Fisher Scientific, USA) was used to examine DNA concentration and purity. Bacterial 16S rRNA gene high-throughput sequencing was applied to reveal the microbial community structure. Detailed testing methods are provided in Section S3 of Appendix A.

Network analysis was performed to determine the microbial interactions among the bacterial communities recovered from the foulants. An online platform[‡] [37] was used to create networks at the operational taxonomic unit (OTU) level for each group. The topological indexes and the roals of OTUs in microbial networks are shown in Tables S2 and S3 in Appendix A, respectively. Furthermore, a null-model-based framework [38] was used to obtain the contributions of ecological processes to community assembly, and the analysis was performed in an online pipeline.[§] The ecological processes govern the community assembly is shown in Table S4 in Appendix A. Detailed construction methods for network and community assembly analyses are provided in Section S3.

[‡] https://ieg4.rccc.ou.edu/mena/login.cgi.
[§] https://mem.rcees.ac.cn:8080.

2.5. Scaling and particulate fouling assessment

Freeze-dried foulants were ground by a grinding machine (YM-48LD; Yuming, China). The mineral composition of the foulants was determined by means of an X-ray diffractometer (Empyrean; Malvern Panalytical, UK). The General Structure and Analysis System (GSAS) was used to determine the fraction of crystals formed due to mineral scaling and particulate fouling [39]. Here, it should be mentioned that scaling is caused by the formation of chemical precipitations, whereas particulate fouling is caused by the sedimentation and flocculation of particles in wastewater [12].

2.6. Statistical analysis

Significant differences in dry weights, EPS contents, precipitates and particulate contents, and microbial richness between the groups were determined by one-way analysis of variance (ANOVA). Non-metric dimensional scaling (NMDS) was constructed to evaluate the similarity among microbial communities. Analysis of similarities (ANOSIM) and permutational multivariate analysis of variance (PERMANOVA) were applied to determine the significance among microbial communities. Spearman analyses were used to evaluate the correlations between the abundances of OTUs, microbial diversities, EPS contents, and contents of particulates and precipitates. The relationships between water quality and NBs properties and various foulants were also investigated by means of Spearman analyses. Structural equation model analysis (SEMA) was applied to determine the direct and indirect effects of NBs on fouling using AMOS software (v.22.0; IBM, USA).

3. Results

3.1. Control capacity of NBs for various types of foulant

The results of NBs treatment for fouling prevention using different gas NBs and at different concentrations are shown in Fig. 2(a). In comparison with the controls (CK, non-NB), treatments with saturated NBs (100% concentration) significantly reduced the total foulant dry weights by 37.7%–64.1%. A comparison of effectiveness by gas type showed that O_2_100% NBs had higher antifouling capacities than N_2_100% and He_100% NBs. However, these values were only statistically significant ($p < 0.05$) over 600 h. In addition, N_2_100% NBs showed a higher but not significant ($p > 0.05$) antifouling capacity than He_100% NBs. This result suggests that the physical properties of the NBs—rather than the chemical properties of oxygen gas—are more responsible for fouling control.

The concentration of O_2_NBs in the water affected the antifouling effectiveness. Compared with CK, water containing more than 50% saturated O_2_NBs (O_2_50%, O_2_75%, O_2_100%) exhibited a significant ($p < 0.05$) reduction in total foulants by 8.0%–64.1% (Fig. 2(a)). Water containing less than 50% saturated O_2_NBs lacked antifouling capacity. O_2_5% water significantly ($p < 0.05$) increased the total fouling by 12.2%–22.7%. There were no significant differences in fouling content between the CK and O_2_25% treatments.

The application of NB-infused water to pipes that had an existing fouling layer did not significantly ($p > 0.05$) remove the attached fouling at the end of a 24-h period (Fig. 2(b)). This result suggests that NBs have the ability to prevent fouling formation, but their physical shear stresses cannot remove a preformed fouling layer.

The ability of NBs to control biofouling, scaling, and particulate fouling was further investigated. In comparison with CK, the microbial quantity (Fig. 2(c)), EPS content (Fig. 2(d)), precipitates (Fig. 2(e)), and particulates (Fig. 2(f)) in treatments with saturated NBs were significantly ($p < 0.05$) reduced by 34.4%–59.5%, 32.6%–55.6%, 27.9%–76.7%, and 40.9%–61.4%, respectively. Furthermore, the concentrations of O_2_NBs affected the antifouling ability. For example, the O_2_5% and O_2_25% treatments aggravated biofouling, with the microbial quantities and EPS contents increasing by 9.8%–46.3% and 7.9%–36.9%, respectively. These values were statistically significant ($p < 0.05$) in most cases. In contrast, the O_2_50%, O_2_75%, and O_2_100% treatments significantly ($p < 0.05$) mitigated biofouling.

The O_2_5% treatment significantly ($p < 0.05$) increased inorganic precipitates, while the O_2_50%, O_2_75%, and O_2_100% treatments significantly ($p < 0.05$) reduced precipitates by 16.3%–76.7%. For particulate fouling, all NBs treatments reduced the particulate content by 5.7%–61.4%. These values were statistically significant ($p < 0.05$) when the NBs concentrations were greater than 50%. Overall, higher O_2_NBs concentrations had better anti-particulate fouling control efficiency.

The antifouling capacity decreased sharply when the O_2_NBs concentration dropped below 50% saturation; in contrast, there was little difference when the O_2_NBs concentration was greater than 50% saturation. No significant differences were found in fouling weights between the O_2_75% and O_2_100% groups in most comparisons. Moreover, it was found that, as the experimental time increased, the NBs antifouling capacity decreased (Fig. S2 in Appendix A). For example, NBs eliminated 44.7%–64.1% of the total foulants in the first 300 h, but this value decreased to 37.7%–54.4% before the experiment was concluded after 900 h. More specifically, in comparison with scaling and particulate fouling, the NBs control efficiency for biofouling decreased more rapidly over time. In addition, the SEM results revealed that the fouling layer in pipes exposed to a continuous flow of NB-infused water had a looser structure than those in the control treatment (Fig. 2(g)), which could be attributed to the collapse of NBs.

3.2. Effects of NBs on biofouling

16S rRNA gene sequencing of the microbial community in the composite foulants retrieved sufficient gene sequences for meaningful data analysis (Fig. S3 in Appendix A). All saturated NBs treatments greatly reduced microbial diversity, as evidenced by a significant ($p < 0.05$) reduction in the Shannon indices (Fig. 3(a)), particularly in the O_2_NB-treated groups. However, the O_2_5% treatment significantly ($p < 0.05$) increased community diversity. The major phyla identified in the foulants (Fig. 3(b)) were Firmicutes (19.6%–61.2%), Proteobacteria (22.6%–47.3%), Actinobacteria (6.5%–19.5%), and Bacteroidetes (2.0%–11.1%). The NBs significantly shifted the composition of these communities. For example, NBs reduced the abundance of Firmicutes by 2.6% to 25.4%, while increasing the abundance of Proteobacteria. Nonmetric multidimensional scaling (NMDS) (Fig. S4 in Appendix A) suggested that the communities treated by different NBs types and concentrations were clearly separated. Furthermore, ANOSIM (Figs. S5 and S6 in Appendix A) and PERMANOVA (Table S5 in Appendix A) showed that the microbial communities within the groups varied significantly ($p < 0.05$). The community structure also changed over time; for example, Firmicutes and Proteobacteria clearly decreased and increased, respectively, in abundance over time.

The network analysis results (Figs. 3(c)–(j)) showed that O_2_50%, O_2_75%, and saturated NBs (100%) simplified the microbial networks (see Table S6 in Appendix A for the topological properties of the networks). In these treatment groups, the total links, average connectivity, and clustering coefficients were lower than those in the controls, while the average path distances and modularity were higher. In contrast, the O_2_5% and O_2_25% treatments increased network complexity. For example, the total links increased by 9.8%–33.4% in the two groups. The topological properties of the nodes in the networks (Fig. S7 and Table S7 in Appendix A) indi-

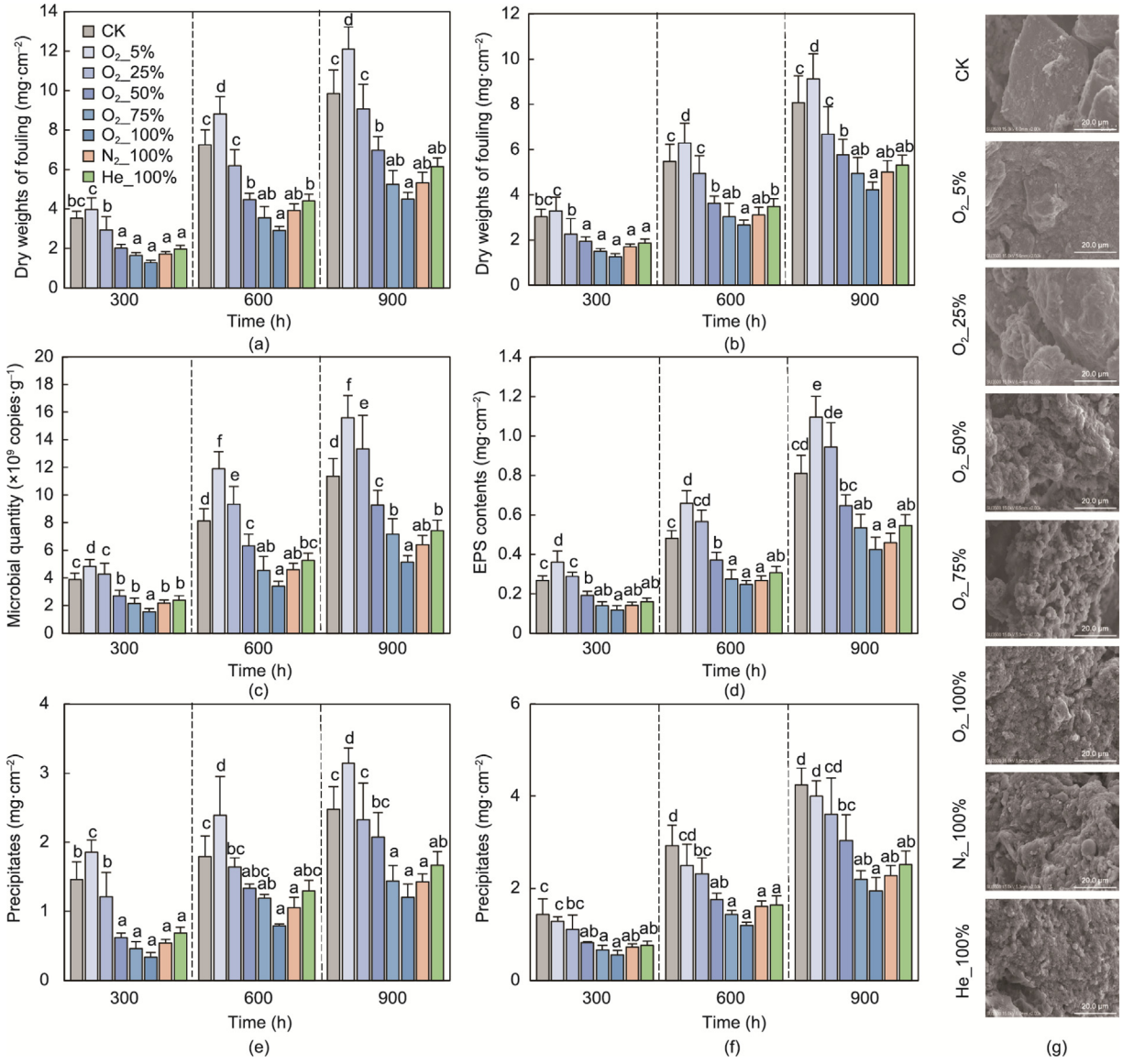

Fig. 2. Analyses of foulant dry weights and composition during different NBs treatments. The treatment scheme is depicted by different colors in (a) showing foulant dry weights at three timepoints under continuous NBs treatment (prevention strategy). (b) Dry weights of foulants from pre-fouled pipes subjected to 24 h shock treatment for foulant removal. Since NBs did not remove preexisting fouling, only this figure shows the result of the removal strategy. (c–f) The contents of microbes, EPS, precipitates, and particulates in the foulant, as indicated by the y-axis labels. Error bars indicate standard deviations, and the letters on top of the bars indicate significantly different groups based on statistical analysis. The composition analyses were only performed for the continuous NBs treatment experiments. (g) Foulant morphology and composition revealed by SEM for foulants collected at 900 h. The letters above the boxplots indicate significant analysis, treatments that have the same letter indicate not significant.

cated that generalist OTUs were significantly lower in the saturated NBs treatments. The O_2_50% and O_2_75% treatments also reduced the total numbers of generalist OTUs, whereas the O_2_5% and O_2_25% treatments increased the total numbers.

Examinations of the ecological processes of the microbial community assemblies (Fig. S8 in Appendix A) revealed that saturated NBs treatments increased the absolute β nearest-taxa index (βNTI) of the communities, indicating an enhancement in community deterministic assembly processes. βNTI responded differently to treatments with different O_2_NBs concentrations; the absolute value of βNTI decreased in the O_2_5% treatment groups (enhanced stochastic processes), whereas 25%–100% NBs increased the absolute values (enhanced deterministic processes). The main ecological process for the O_2_5% treatment group was homogenizing dispersal, whereas for other groups—particularly at higher NBs concentrations—the homogeneous selection was dominant in governing the communities.

3.3. Effects of NBs on scaling and particulate fouling

X-ray diffraction (XRD) patterns (Fig. S9 (a) in Appendix A) showed that the foulants contained four types of precipitates (i.e., calcite, aragonite, monohydrocalcite, and dolomite) and four types of particulates (i.e., quartz, muscovite, feldspar, and chlorite). Quartz (accounting for 18.6%–33.2%), muscovite (10.5%–15.3%), feldspar (8.2%–14.2%), and calcite (25.5%–49.4%) were the main minerals (Fig. S9 (b) in Appendix A).

The effects of NBs treatments on different types of precipitates are shown in Figs. 4(a)–(d). In general, the NBs reduced calcite by 10.2%–80.9% and monohydrocalcite by 13.1%–83.5%, except in the experiments with O_2_5%, which showed an increase in both. In contrast, all NBs treatments significantly increased the aragonite content by 69.9%–325.1%. Because calcite and aragonite are different crystalline forms of $CaCO_3$, the results suggest that the NBs aided in the transition from calcite to aragonite. In addition, the

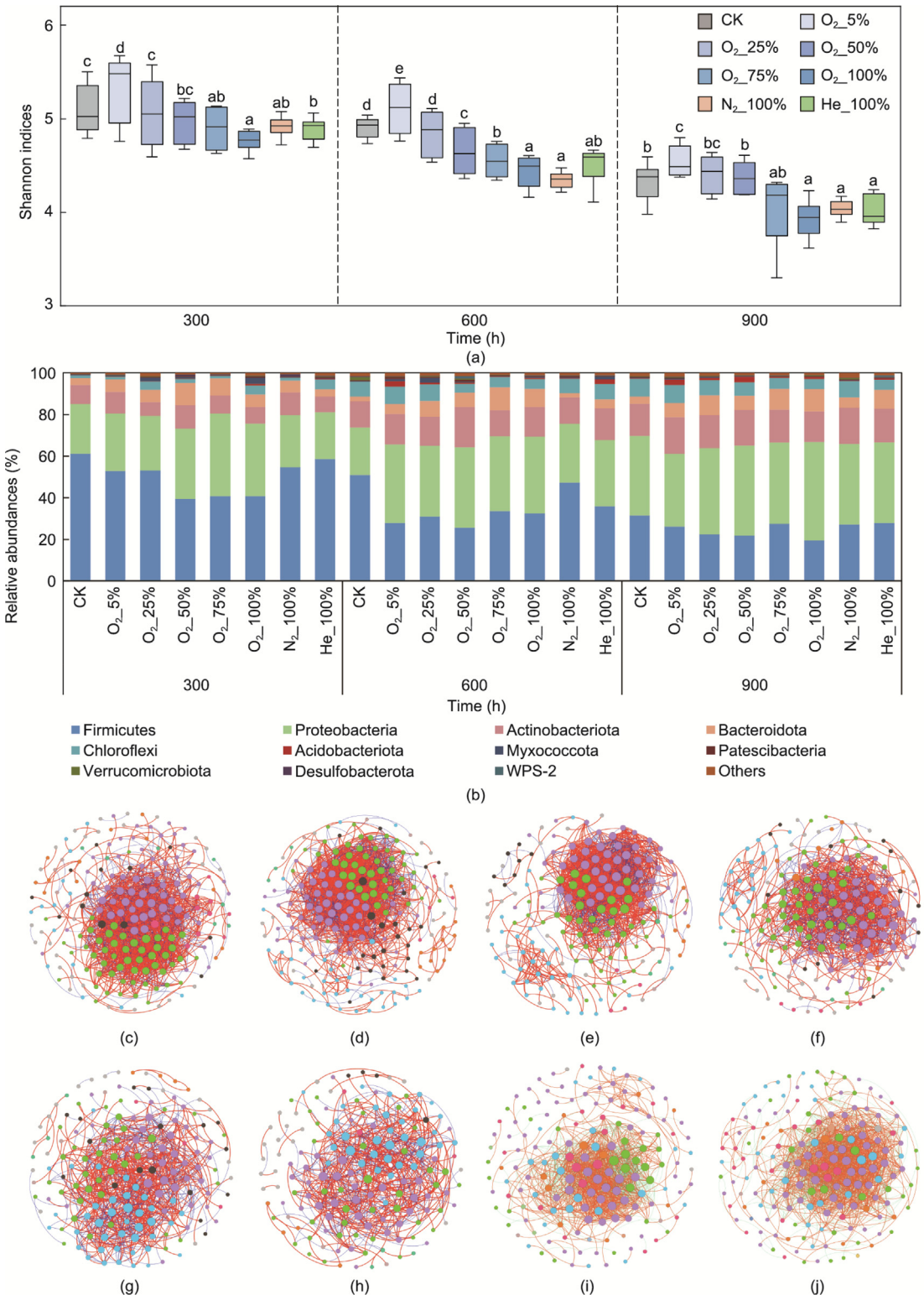

Fig. 3. Diversity, composition and network of microbial communities. (a) Shannon indices, the letters above the boxplots indicate significant analysis, treatments that have same letter indicate not significant. (b) Microbial compositions at the phylum level. (c–j) represent the control (CK), O_2_5%, O_2_25%, O_2_50%, O_2_75%, O_2_100%, N_2_100%, and He_100% microbial networks, respectively. The red line represents a positive relationship, and green represents a negative relationship; nodes with different colors represent different modules.

NBs reduced the content of dolomite in the foulants by 27.5%–74.4%.

Figs. 4(e)–(h) shows that all NBs treatments inhibited the formation of particulates on pipe surfaces. The quartz content was reduced by 15.0%–61.2%, muscovite was reduced by 7.2%–64.5%, feldspar was reduced by 2.9%–57.7%, and chlorite was reduced by 3.6%–68.7%. Moreover, higher concentrations of NBs had higher efficiencies in reducing particulate fouling.

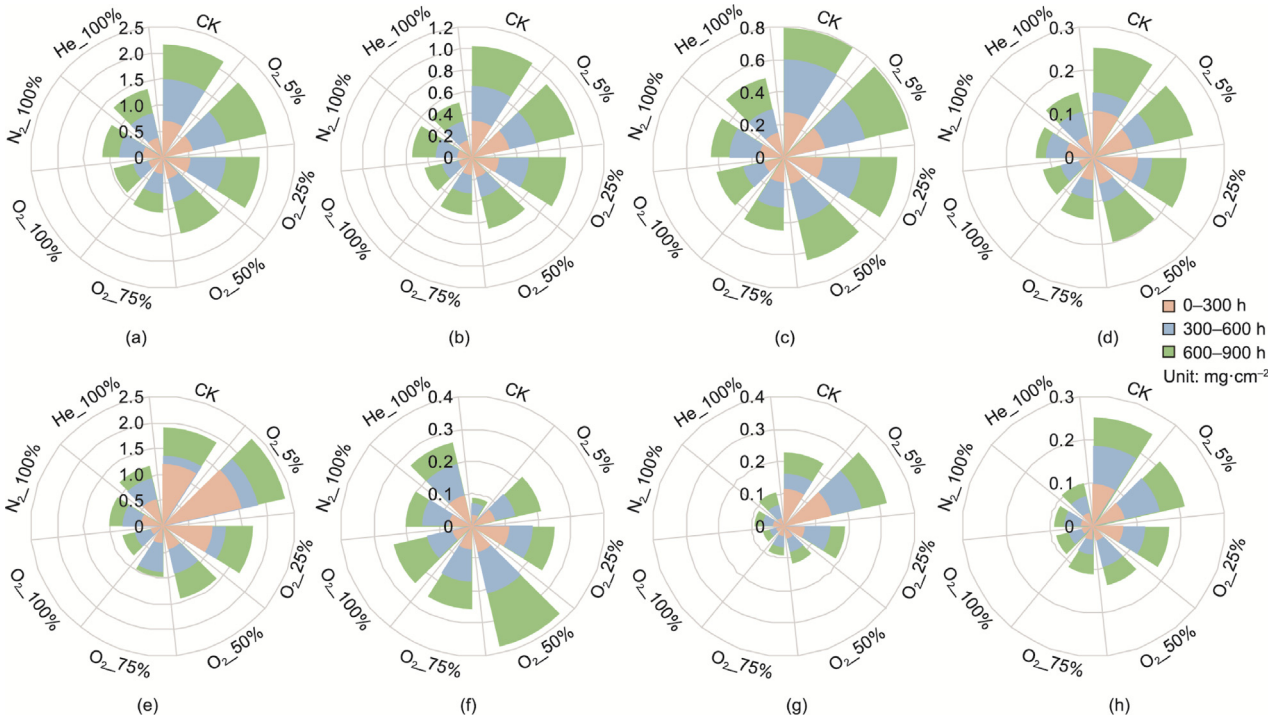

Fig. 4. Analyses of precipitates and particulates in foulants. Minerals are depicted by colored radio bars for (a) quartz, (b) muscovite, (c) feldspar, (d) chlorite, (e) calcite, (f) aragonite, (g) monohydrocalcite, and (h) dolomite. Radio graphs illustrate the mineral content ($mg \cdot cm^{-2}$) by different treatments (eight groups as labeled on the outside ring). The mineral content collected at three different time points is depicted by the color legend on the right.

3.4. NBs properties and their effects on water quality

NBs application was found to change the bubble properties (Fig. S10 in Appendix A). NBs-saturated water had 6.5–9.2 times higher bubble concentrations than the controls, the mean bubble size increased by 7.2%–52.7%, and the D10 and D50 sizes increased by 2.4%–15.2% and 9.3%–48.2%, respectively. Furthermore, NBs infusion reduced the SSAs of the bubbles by 6.7%–34.5%.

NBs infusion also altered the water quality (Fig. 5(a)). The pH of the NB-infused water increased by 0.01–0.30 relative to that of the controls. The EC and water ST increased by up to 17.5% and 13.6%, respectively. However, the changes in water pH, EC, and ST were not statistically significant. The NBs also significantly ($p < 0.05$) increased the absolute values of the water ZP. Conversely, the NBs reduced the COD by 3.8%–27.3% and the BOD by 4.4%–23.9%. The changes in COD and BOD were statistically significant ($p < 0.05$) when the NBs concentrations were higher than 50%. Furthermore, O_2_100% had the greatest influence on the water quality parameters.

In terms of microorganisms, NBs significantly ($p < 0.05$) activated microbial growth at O_2_5%, while higher NBs concentrations reduced the microbial quantities by 10.4%–31.8%. This finding could be related to the disinfection property of ·OH generated during NBs collapse (Fig. 5(b)). ·OH were detected when the NBs concentration was greater than O_2_25% and increased with increasing NBs concentrations. No ·OH were found in the control and O_2_5% waters; thus, no disinfection occurred. In addition, O_2_NBs generated more ·OH than the inert gas NBs. It was found that the bubble properties have close connections with water quality (Fig. S11 in Appendix A). For example, NBs concentrations had significant ($p < 0.05$) positive correlations with water pH, ST, and ORP, while both the highest intensity of the ESR patterns and the NBs concentrations had significant ($p < 0.05$) negative correlations with water COD, BOD, and AHPC. In addition, the mean size, D10 size, and D50 size of NBs had significant interactions with some water parameters. The results suggest that the water quality changes were strongly associated with the NBs properties and hydroxyl radicals. Furthermore, correlation analyses indicated that the microbial quantity was positively correlated with COD and BOD (Fig. 5(c)), suggesting that the water quality parameters influenced each other.

3.5. NBs fouling control pathways

Significant correlations were found between water quality and the various foulants (Fig. S12 in Appendix A). More specifically, the foulant dry weights had a significant negative relationship with water pH and ST but a positive relationship with COD and BOD. The results indicate that changes in water quality are important for foulant reduction. In addition, various foulants were correlated with each other (Fig. S13 in Appendix A): Significant interactions were found between EPS contents and several mineral types (e.g., calcite, quartz, and dolomite). Several key bacteria in the networks were also significantly correlated with minerals.

Based on the correlations, a SEMA (Fig. 6) was applied to reveal the direct and indirect antifouling pathways of NBs. The SEMA showed that the NBs directly and significantly affected biofilms, salt precipitates, and particulates, as indicated by the standardized path coefficient (SPC) values, which ranged from −0.56 to −0.72. Moreover, the significant correlations found between water quality and the various foulants suggest that NBs also mitigate fouling indirectly by affecting water quality (SPC = −0.43). Furthermore, the precipitates (SPC = 0.52) and particulates (SPC = 0.41) had greater impacts on the foulant weights than the biofilms (SPC = 0.13), which had a minor impact. Interactions among various types of foulants could be another factor influencing NBs anti-fouling. For example, since both the precipitates and the particulates had significant ($p < 0.05$) positive interactions with biofilms, it can be concluded that the reduction in biofilms in the NBs groups could indirectly lead to a reduction in precipitates and particulates.

Parameter	CK	O_2_5%	O_2_25%	O_2_50%	O_2_75%	O_2_100%	N_2_100%	He_100%
pH	8.0 ± 0.3 a	8.0 ± 0.2 a	8.1 ± 0.2 a	8.1 ± 0.3 a	8.2 ± 0.2 a	8.3 ± 0.3 a	8.3 ± 0.3 a	8.2 ± 0.3 a
ST ($\times 10^{-3}$ N·m^{-1})	83.3 ± 9.3 a	84.7 ± 7.9 a	89.4 ± 11.2 a	91.5 ± 10.4 a	92.6 ± 8.6 a	97.9 ± 10.1 a	96.0 ± 9.4 a	94.8 ± 7.7 a
EC (ds·m^{-1})	2.2 ± 0.2 a	2.0 ± 0.2 a	2.1 ± 0.2 a	2.1 ± 0.2 a	2.2 ± 0.3 a	2.4 ± 0.2 a	2.4 ± 0.3 a	2.5 ± 0.2 a
ORP (mv)	−37.1 ± 37.3 a	29.8 ± 21.2 b	67.0 ± 29.5 b	76.1 ± 31.6 b	80.2 ± 27.4 b	83.2 ± 31.2 b	49.4 ± 32.5 b	88.8 ± 29.7 b
COD (mg·L^{-1})	410.0 ± 76.3 a	394.6 ± 64.2 a	371.1 ± 63.1 a	354.4 ± 56.3 ab	320.3 ± 58.2 b	297.9 ± 52.7 b	348.9 ± 61.8 ab	339.2 ± 68.3 b
BOD (mg·L^{-1})	135.1 ± 23.5 a	129.1 ± 15.7 a	124.5 ± 15.4 a	115.3 ± 10.6 b	110.4 ± 9.5 b	102.8 ± 18.3 b	116.0 ± 18.6 b	113.8 ± 20.3 b
ZP (mv)	−6.9 ± 2.9 d	−26.7 ± 3.5 b	−32.5 ± 3.2 ab	−35.4 ± 5.7 ab	−39.2 ± 5.3 a	−41.0 ± 4.4 a	−12.9 ± 3.3 cd	−18.1 ± 3.0 c
AHPC ($\times 10^3$ CFU·mL^{-1})	3.4 ± 0.5 b	3.9 ± 0.6 b	3.5 ± 0.8 b	3.1 ± 0.9 b	2.6 ± 0.6 c	2.3 ± 0.5 c	3.0 ± 0.8 c	2.8 ± 0.7 a

(a)

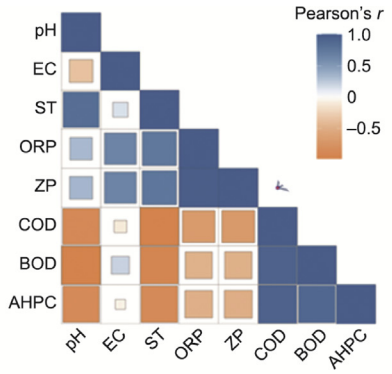

(c)

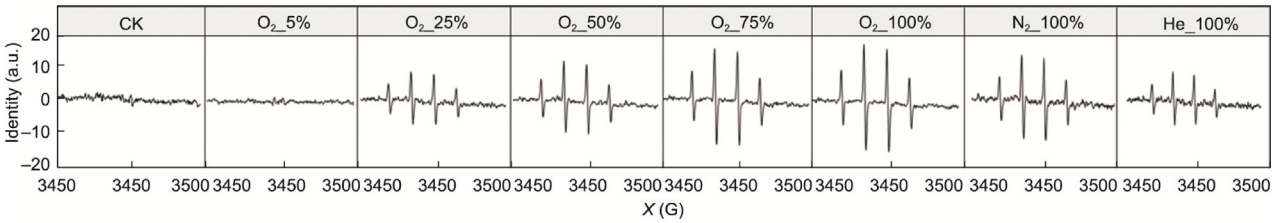

(b)

Fig. 5. Water quality and their relationships in different NBs experimental groups. (a) Water quality in different experiment groups, including water pH, EC, ST, oxidation reduction potentials ORP, ZP, COD, BOD, and AHPC, the letters indicate significant analysis, treatments that have same letter indicate not significant. (b) Electron spin resonance (ESR) signal patterns of hydroxyl radicals. (c) Correlation among various water quality parameters (the strength of the correlation is depicted by the color scale on the right). *X*: magnetic field; CFU: colony forming unit.

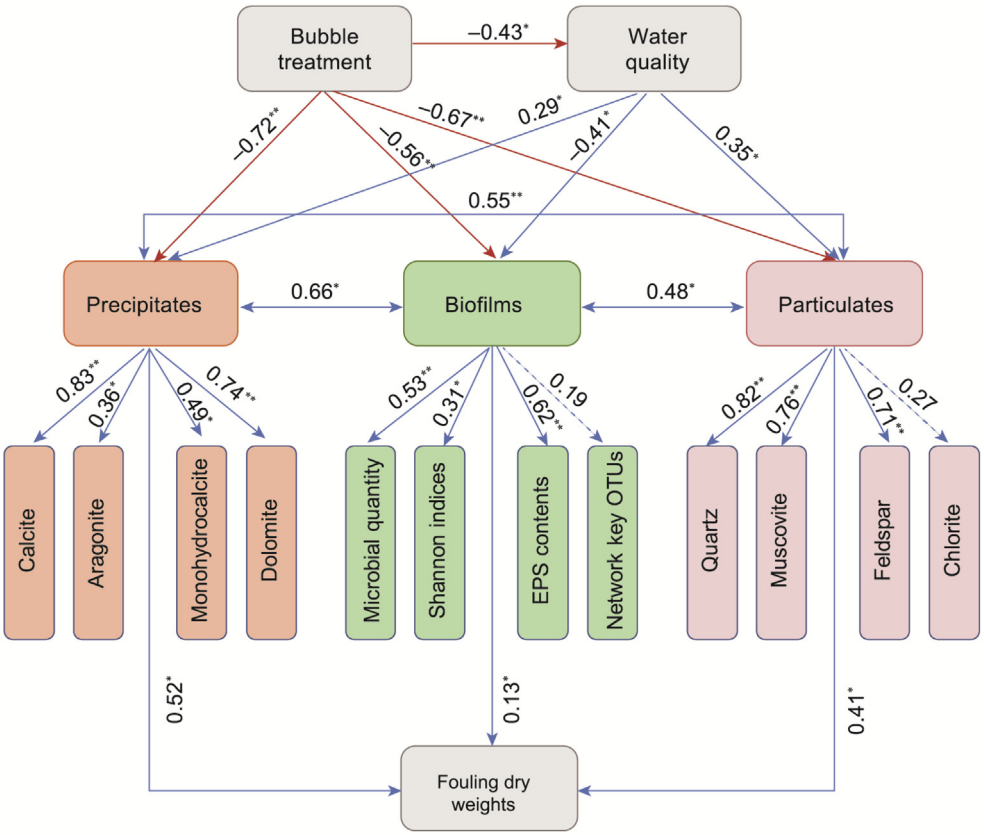

Fig. 6. Controlling pathways of NBs on composite fouling revealed by structural equation model. The results were calculated based on the data from control group and prevention strategy treatments, i.e., including CK, O_2_5%, O_2_25%, O_2_50%, O_2_75%, O_2_100%, N_2_100%, and He_100%. Adjacent numbers represent the standardized regression weights; water quality was the dimension reduction from pH, ST, ORP, COD, BOD, and ZP; red line represents negative and blue line is positive relationship. Chi-square ($\chi 2$) / degree of freedom (df) = 2.51, goodness-of-fit index (GFI) = 0.928, nonsignificant probability level (P) = 0.34. * and ** represent $p < 0.05$ and $p < 0.01$.

4. Discussion

4.1. Control capacity of NBs for various types of foulant

The results of this study showed that all the saturated NBs effectively inhibited composite fouling. A comparison of different types of gas showed that the oxygen NBs did not significantly improve fouling control. Although oxygen NBs were more useful in reducing biofouling, no significant ($p > 0.05$) differences were found between oxygen NBs and inert gases NBs in reducing scaling and particulate fouling. Because of the high proportion (>70%) of scaling and particulate fouling in the total amount of foulants, different types of NBs had similar antifouling effects. The results suggest that the internal gas used to generate NBs did not significantly contribute to composite fouling reduction. Instead, the physical and chemical properties of the NBs are likely to be important for fouling mitigation. Based on these results, plausible antifouling mechanisms of NBs are illustrated in Fig. 7.

NBs simultaneously act as biocides and activators for microorganisms (Fig. 7(a)). Their biocidal activity is attributed to the ·OH generated by NBs collapse; ·OH has been recognized as a strong oxidant for bacterial inactivation and organic oxidation [18]. This observation agrees with several other studies that have reported the disinfection capacity of NBs [18,19,40,41]. The mechanisms of microbial activation via NBs have not been fully elucidated, although a few studies [42,43] have reported enhanced microbial growth. One possible explanation is that NBs (e.g., oxygen and air NBs) provide microorganisms with more oxygen, accelerating their growth rate. However, Ito and Sugai [43] found that CO_2 NBs also activated microorganisms, implying that O_2 is not the only factor that causes enhanced microbial growth. These researchers proposed that the negatively charged NBs attracted cations at the gas–liquid interfaces, increasing the rate of proton transfer to the microorganisms and thereby activating the microorganisms. NBs concentrations were found to influence the inhibition or activation effects of NBs on microorganisms (Fig. S14 in Appendix A). The activation effects of NBs were predominant at low concentrations (5% O_2 to 25% O_2), whereas the inhibition effects of NBs were predominant at high concentrations (50% O_2 to 100% O_2), with a high concentration of ·OH and resulting in a net inactivation effect at high NBs concentrations. In addition, although ·OH radicals play a significant role in reducing microorganisms and biofouling, they appear to be ineffective at directly reducing chemical fouling and particulate fouling. In other words, ·OH was found to be effective for mitigating biofouling but not for reducing composite fouling.

In terms of NBs gas types, saturated O_2 NBs outperformed the two types of inert gases in terms of water sterilization and biofouling mitigation. This is because the O_2 NBs generated more ·OH (Fig. 5). NBs collapse causes a sharp increase in the local pressure and temperature [44], increasing the energy at the gas-liquid interface, which decomposes oxygen molecules, resulting in higher production of ·OH [45]. The presence of oxygen molecules can help to generate more ·OH. This observation agrees with earlier studies reporting that O_2 NBs generate more ·OH than N_2 NBs [46], and that O_2 NBs are more effective in killing *Vibrio parahaemolyticus* than air NBs [30].

NBs fouling control was also reflected in the alteration of the microbial community. The O_2_5% NBs treatment increased the microbial diversity (Fig. 3) because the NBs application enhanced the O_2 available to microorganisms [47], which increased the stochastic processes of community assembly. In contrast, high concentrations of NBs probably acted as a stressor, selecting microorganisms resistant to NBs and ·OH [3], and thereby reducing community diversity and enhancing the deterministic processes of community assembly. Furthermore, the NBs altered the co-occurrence patterns of the microorganisms. The total links, connectivity, and generalist OTU numbers increased with the O_2_5% and O_2_25% NBs treatments. In general, higher complexity, connectivity, and stability of community networks will aid in biofilm growth [48,49]; thus, low concentrations of NBs promoted biofouling. In contrast, the opposite phenomena were observed when the O_2 NBs concentrations ranged between 50% and 100% (decreased network sizes, links, and connectivity), implying that the NBs inhibited the transmission efficiency of energy, matter, and interactions between microorganisms [50], thereby inhibiting the development of biofouling [51].

The mechanisms for the reduction in salt precipitates by NBs are illustrated in Fig. 7(b). First, because NBs are negatively charged, cations (e.g., Ca^{2+} and Mg^{2+}) are easily attracted to their gas–liquid interfaces [28], which reduces the probability of contact between cations and anions. As a result, the NBs act as chelators inhibiting precipitate formation. Second, the negative gas-liquid interfaces of the NBs attract protons (i.e., H^+); this promotes the transformation of HCO_3^- to CO_3^{2-}, shortening the crystallization induction period and resulting in accelerated aragonite formation and reduced calcite formation. Since aragonite has a looser structure than calcite, it can be easily flushed out with water flow [52]. However, O_2_NBs was found to enhance scaling when the treatment concentration was less than 25%. The increased scaling observed is likely related to accelerated biofilm growth due to the microbial activation effect of NBs at low concentrations, since biofilms and precipitates were positively and significantly correlated. Previous studies have demonstrated that the ionizable functional groups of biofilms can serve as efficient nucleation sites for precipitates [53], significantly accelerating the formation of precipitates [54]. Therefore, the growth of biofilms triggered by low concentrations of NBs indirectly increased mineral precipitation by enhancing the biomineralization capacity of the biofilms. Furthermore, because of the interactions between the biofilms and precipitates, high concentrations of NBs may have indirectly impaired precipitate growth by lowering the biofilm's biomineralization ability. As a result, when NBs are present in high concentrations, the production of ·OH could be a plausible mechanism for precipitate reduction.

The NBs also effectively mitigated particulate fouling. In general, the interactions between particles are governed by electrostatic interactions, van der Waals forces, and hydrophobic forces [55]. The bulk of wastewater particles are negatively charged. Cationic polymeric coagulants are used to destabilize particles and minimize electrostatic repulsion, thereby assisting in the production of aggregate flocs and enhancing particle separation from wastewater [22,56,57]. The water quality analysis showed fewer particles in the wastewater infused with NBs (Fig. S15 in Appendix A), suggesting that the mitigation of particulate fouling was due to the promotion of particle aggregation by the NBs. Negatively charged NBs surfaces form gas bridges, promoting the aggregation of particles. This process is similar to dissolved air flotation technology (DAFT), which operates by releasing gas-supersaturated pressurized water into atmospherically pressurized water, in which bubbles—including nanobubbles—spontaneously form. These bubbles aid in removing suspended particles from wastewater [58]. Fig. 7(c) illustrates how the NBs surfaces combine to form "bridges" between particles, thereby serving as coagulants to remove wastewater particles. Furthermore, as the NBs concentrations increased, the absolute water of the water ZP increased (Fig. 5(a)), indicating that the NBs have a strong ability to act as particle "bridges" and promote particle coagulation or flocculation, thereby reducing the content of particles in wastewater and increasing the anti-particulate fouling capacity.

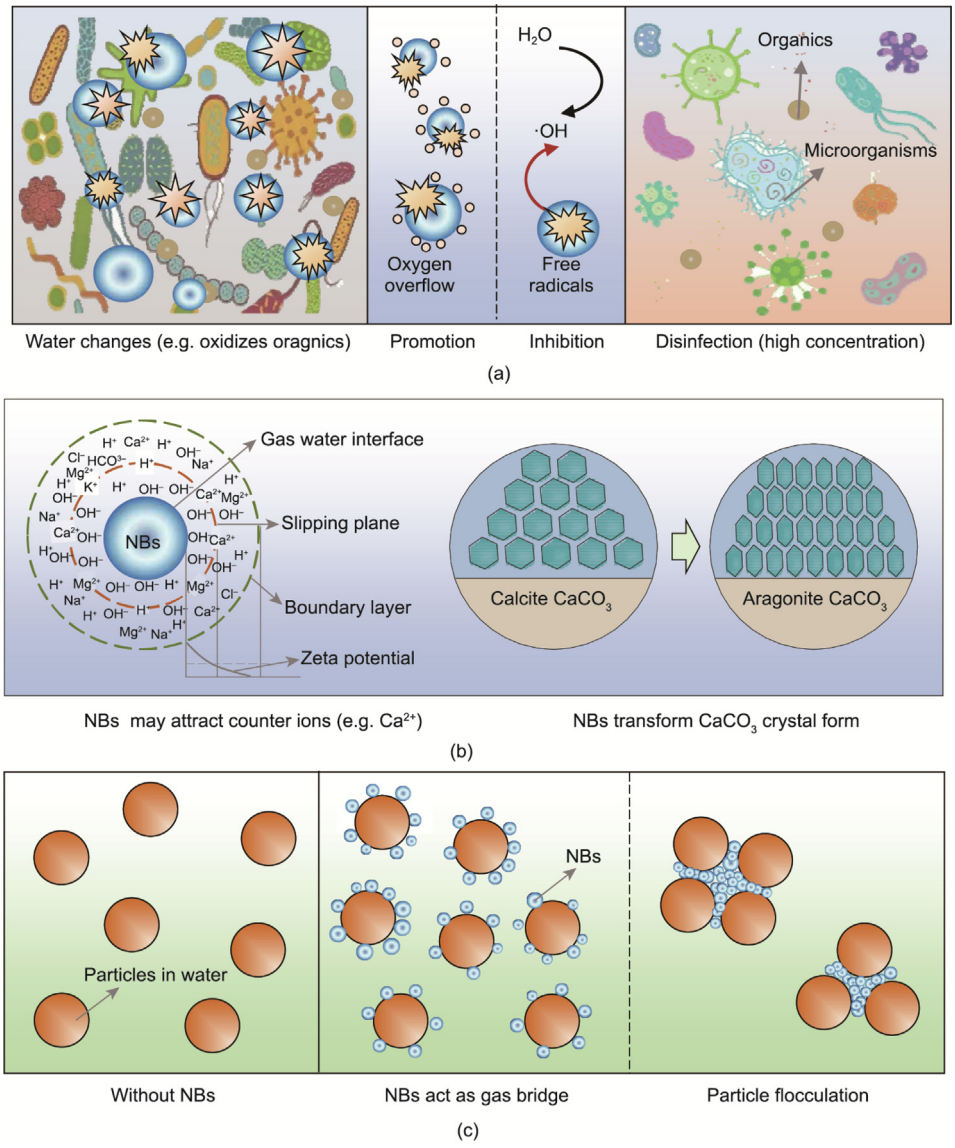

Fig. 7. Illustration of nanobubbles antifouling mechanisms. (a–c) represent the control mechanisms for biofouling, scaling and particulate fouling, respectively.

4.2. Engineering implications

Despite the effectiveness of NBs in controlling fouling, detailed guidance is needed to improve their engineering applications. The selection of gases for NBs generation is the first design consideration. O_2 NBs have higher but statistically nonsignificant antifouling capacities relative to inert gases (N_2 and He) in most comparisons. The production cost of pure O_2, N_2, and He NBs is higher than that of air (21% O_2 and 78% N_2) NBs. Furthermore, the antifouling capacity of air NBs may be comparable to that of O_2 and N_2 NBs. Therefore, air NBs are the best option for economical fouling mitigation in most wastewater distribution systems. However, for agricultural wastewater irrigation applications, O_2 NBs-infused water is already commonly applied to increase the oxygen content in the bonded soil [32,33]. In comparison with inert gas NBs, which cannot be used for crops, O_2 NBs can boost agricultural production and quality while simultaneously increasing economic benefits. These benefits may be higher than the production cost of O_2 NBs [59]. Furthermore, because the effects of O_2 NBs-infused water on crop growth vary depending on crop type [32,33] and O_2 concentration [60], there should be a tradeoff between the cost of O_2 NBs generation and the increase in economic benefit.

The selection of NBs concentrations may be the second design criterion. Low-concentration NBs activated microbial growth, which aggravated biofouling and scaling. Therefore, the NBs concentrations used for mitigating biofouling should be higher than a 50% gas saturation concentration. Moreover, it was found that the O_2_75% and O_2_100% NBs did not have obvious differences in mitigating various foulants. Thus, NBs with an approximately 75% gas saturation concentration are recommended for controlling biofouling and scaling. For particulate fouling, higher NBs concentrations had higher mitigation efficiencies. Therefore, the selection of NBs concentration should consider both the influent and the required effluent water quality for fouling mitigation. Moreover, it is worth noting that higher particle-size NBs had a stronger impact on water quality (Fig. S11). In general, the smaller the particle size of bubbles is, the more stable the bubbles are, making them less prone to collapse [61]. In contrast, large-particle NBs are more likely to collapse and generate free radicals, enhancing the effects of the NBs on water quality and antifouling.

The selection of continuous (i.e., prevention strategy) versus intermittent (i.e., removal strategy) NBs applications is another critical design criterion. Contrary to previous studies indicating that NBs can remove preformed foulants from pipe surfaces [22,56,57], the current study showed that NBs were ineffective at removing various types of foulants (Fig. 2(b)). This result may be attributed to the combined effect of various foulants, which significantly increase the mechanical strength of the fouling layer [24,62] due to the high cohesion of the composite fouling layer in the wastewater distribution systems. This cohesion makes the layer resistant to NBs shear forces. Because the NBs did not remove the pre-attached fouling layers, continuous NBs application is needed to mitigate composite fouling.

Lastly, it is important to note that the fouling mitigation effect weakened with an increase in NBs application times. One possible explanation is that the NBs acted as a stressor—like chlorination—to select microorganisms that were resistant to NBs, causing a lower diversity and higher deterministic strength in the microbial communities (Fig. 3), which then decreased the ability of the NBs to control biofouling. Since biofilms can promote the formation of precipitates and particulates, a weaker controlling efficiency for biofilms leads to a decline in controlling efficiency for mineral precipitates and particle deposition. Consequently, the mitigation ability of NBs for composite fouling gradually deteriorates over time. Thus, other fouling control measures should be combined with NBs treatment in the later stages.

Acknowledgments

Funding support for this research was provided by the National Natural Science Foundation of China (52339004 and 52209074), Natural Science Foundation of Shandong Province (ZR2022QE079), National Key Research and Development Plan (2021YFD1900900), the earmarked fund for CARS-03, and the China Post-doctoral Science Foundation (BX2021363 and 2022M713394). Sunny C. Jiang was supported by US National Science Foundation (CBET 2027306, CBET 2128480, and CBET 1806066), US Bureau of Reclamation (R21AC10079-00), and US Environmental Protection Agency (EPA-G2021-STAR-A1, 84025701).

Compliance with ethics guidelines

Yang Xiao, Bo Zhou, Siyuan Tan, Lei Li, Tahir Muhammad, Buchun Si, Changjian Mad, Sunny C. Jiang, and Yunkai Li declare that they have no conflict of interest or financial conflicts to disclose.

Appendix A. Supplementary material

Supplementary data to this article can be found online at https://doi.org/10.1016/j.eng.2023.10.013.

References

[1] Rho H, Im SJ, Alrehaili O, Lee S, Jang A, Perreault F, et al. Facile surface modification of polyamide membranes using UV-photooxidation improves permeability and reduces natural organic matter fouling. Environ Sci Technol 2021;55(10):6984–94.
[2] Tran QK, Jassby D, Schwabe KA. The implications of drought and water conservation on the reuse of municipal wastewater: recognizing impacts and identifying mitigation possibilities. Water Res 2017;124:472–81.
[3] Xiao Y, Jiang SC, Wang XY, Muhammad T, Song P, Zhou B, et al. Mitigation of biofouling in agricultural water distribution systems with nanobubbles. Environ Int 2020;141:105787.
[4] Singh A. A review of wastewater irrigation: environmental implications. Resour Conserv Recycling 2021;168:105454.
[5] Wang J, Wang L, Sun N, Tierney R, Li H, Corsetti M, et al. Viscoelastic solid-repellent coatings for extreme water saving and global sanitation. Nat Sustain 2019;2(12):1097–105.
[6] Wang M, Zhang P, Liang X, Zhao J, Liu Y, Cao Y, et al. Ultrafast seawater desalination with covalent organic framework membranes. Nat Sustain 2022;5(6):518–26.
[7] Seo DH, Pineda S, Woo YC, Xie M, Murdock AT, Ang EYM, et al. Anti-fouling graphene-based membranes for effective water desalination. Nat Commun 2018;9(1):683.
[8] Im SJ, Fortunato L, Jang A. Real-time fouling monitoring and membrane autopsy analysis in forward osmosis for wastewater reuse. Water Res 2021;197:117098.
[9] Desmond P, Huisman KT, Sanawar H, Farhat NM, Traber J, Fridjonsson EO, et al. Controlling the hydraulic resistance of membrane biofilms by engineering biofilm physical structure. Water Res 2022;210:118031.
[10] Wakai S, Eno N, Miyanaga K, Mizukami H, Sunaba T, Miyano Y. Dynamics of microbial communities on the corrosion behavior of steel in freshwater environment. NPJ Mater Degrad 2022;6(1):45.
[11] Schoenitz M, Grundemann L, Augustin W, Scholl S. Fouling in microstructured devices: a review. Chem Commun 2015;51(39):8213–28.
[12] Guo W, Ngo HH, Li J. A mini-review on membrane fouling. Bioresour Technol 2012;122:27–34.
[13] Xiao Y, Liu Y, Ma C, Muhammad T, Zhou B, Zhou Y, et al. Using electromagnetic fields to inhibit biofouling and scaling in biogas slurry drip irrigation emitters. J Hazard Mater 2021;401:123265.
[14] Scarascia G, Fortunato L, Myshkevych Y, Cheng H, Leiknes TO, Hong PY. UV and bacteriophages as a chemical-free approach for cleaning membranes from anaerobic bioreactors. Proc Natl Acad Sci USA 2021;118(37):e2016529118.
[15] Song P, Feng G, Brooks J, Zhou B, Zhou H, Zhao Z, et al. Environmental risk of chlorine-controlled clogging in drip irrigation system using reclaimed water: the perspective of soil health. J Clean Prod 2019;232:1452–64.
[16] Muhammad T, Li L, Xiao Y, Zhou Y, Liu Z, He X, et al. Multiple fouling dynamics, interactions and synergistic effects in brackish surface water distribution systems. Chemosphere 2021;287:132268.
[17] Song P, Zhou B, Feng G, Brooks JP, Zhou H, Zhao Z, et al. The influence of chlorination timing and concentration on microbial communities in labyrinth channels: implications for biofilm removal. Biofouling 2019;35(4):401–15.
[18] Temesgen T, Bui TT, Han M, Kim T, Park H. Micro and nanobubble technologies as a new horizon for water-treatment techniques: a review. Adv Colloid Interface Sci 2017;246:40–51.
[19] Agarwal A, Ng WJ, Liu Y. Principle and applications of microbubble and nanobubble technology for water treatment. Chemosphere 2011;84(9):1175–80.
[20] Azevedo A, Oliveira H, Rubio J. Bulk nanobubbles in the mineral and environmental areas: updating research and applications. Adv Colloid Interface Sci 2019;271:101992.
[21] Farid MU, Kharraz JA, Lee CH, Fang JKH, St-Hilaire S, An AK. Nanobubble-assisted scaling inhibition in membrane distillation for the treatment of high-salinity brine. Water Res 2021;209:117954.
[22] Ghadimkhani A, Zhang W, Marhaba T. Ceramic membrane defouling (cleaning) by air nano bubbles. Chemosphere 2016;146:379–84.
[23] Oppenheimer-Shaanan Y, Sibony-Nevo O, Bloom-Ackermann Z, Suissa R, Steinberg N, Kartvelishvily E, et al. Spatio-temporal assembly of functional mineral scaffolds within microbial biofilms. NPJ Mater Degrad 2016;2:15031.
[24] Shen Y, Huang PC, Huang C, Sun P, Monroy GL, Wu W, et al. Effect of divalent ions and a polyphosphate on composition, structure, and stiffness of simulated drinking water biofilms. NPJ Mater Degrad 2018;4:15.
[25] Ushida A, Hasegawa T, Takahashi N, Nakajima T, Murao S, Narumi T, et al. Effect of mixed nanobubble and microbubble liquids on the washing rate of cloth in an alternating flow. J Surfactants Deterg 2012;15(6):695–702.
[26] Rice D, Westerhoff P, Perreault F, Garcia-Segura S. Electrochemical self-cleaning anodic surfaces for biofouling control during water treatment. Electrochem Commun 2018;96:83–7.
[27] Wu Z, Chen H, Dong Y, Mao H, Sun J, Chen S, et al. Cleaning using nanobubbles: defouling by electrochemical generation of bubbles. J Colloid Interface Sci 2008;328(1):10–4.
[28] Dayarathne H, Jeong S, Jang A. Chemical-free scale inhibition method for seawater reverse osmosis membrane process: air micro-nano bubbles. Desalination 2019;461:1–9.
[29] Wang W, Fan W, Huo M, Zhao H, Lu Y. Hydroxyl radical generation and contaminant removal from water by the collapse of microbubbles under different hydrochemical conditions. Water Air Soil Pollut 2018;229(3):86.
[30] Nghia NH, Van PT, Giang PT, Hanh NT, St-Hilaire S, Domingos JA. Control of Vibrio parahaemolyticus (AHPND strain) and improvement of water quality using nanobubble technology. Aquacult Res 2021;52(6):2727–39.
[31] Xue S, Marhaba T, Zhang W. Nanobubble watering affects nutrient release and soil characteristics. ACS Agric Sci Technol 2022;2(3):453–61.
[32] Chen W, Bastida F, Liu Y, Zhou Y, He J, Song P, et al. Nanobubble oxygenated increases crop production via soil structure improvement: the perspective of microbially mediated effects. Agric Water Manage 2023;282:108263.
[33] Zhou Y, Bastida F, Zhou B, Sun Y, Gu T, Li S, et al. Soil fertility and crop production are fostered by micro-nano bubble irrigation with associated changes in soil bacterial community. Soil Biol Biochem 2020;141:107663.
[34] Puig-Bargues J, Lamm FR, Trooien TP, Clark GA. Effect of dripline flushing on subsurface drip irrigation systems. Trans ASABE 2010;53(1):147–55.
[35] DuBois M, Gilles KA, Hamilton JK, Rebers PA, Smith F. Colorimetric method for determination of sugars and related substances. Anal Chem 1956;28(3):350–6.
[36] Lowry OH, Rosebrough NJ, Farr AL, Randall RJ. Protein measurement with the Folin phenol reagent. J Biol Chem 1951;193(1):265–75.

[37] Kong X, Jin D, Wang X, Zhang F, Duan G, Liu H, et al. Dibutyl phthalate contamination remolded the fungal community in agro-environmental system. Chemosphere 2019;215:189–98.
[38] Stegen JC, Lin X, Fredrickson JK, Chen X, Kennedy DW, Murray CJ, et al. Quantifying community assembly processes and identifying features that impose them. ISME J 2013;7(11):2069–79.
[39] Toby BH, Von Dreele RB. GSAS-II: the genesis of a modern open-source all purpose crystallography software package. J Appl Cryst 2013;46(2):544–9.
[40] Atkinson AJ, Apul OG, Schneider O, Garcia-Segura S, Westerhoff P. Nanobubble technologies offer opportunities to improve water treatment. Acc Chem Res 2019;52(5):1196–205.
[41] Seridou P, Kalogerakis N. Disinfection applications of ozone micro-and nanobubbles. Environ Sci Nano 2021;8(12):3493–510.
[42] Xiao W, Xu G. Mass transfer of nanobubble aeration and its effect on biofilm growth: microbial activity and structural properties. Sci Total Environ 2020;703:134976.
[43] Ito M, Sugai Y. Nanobubbles activate anaerobic growth and metabolism of *Pseudomonas aeruginosa*. Sci Rep 2021;11(1):16858.
[44] Magaletti F, Marino L, Casciola CM. Shock wave formation in the collapse of a vapor nanobubble. Phys Rev Lett 2015;114(6):064501.
[45] Takahashi M, Ishikawa H, Asano T, Horibe H. Effect of microbubbles on ozonized water for photoresist removal. J Phys Chem C 2012;116(23):12578–83.
[46] Li P, Takahashi M, Chiba K. Degradation of phenol by the collapse of microbubbles. Chemosphere 2009;75(10):1371–5.
[47] Sun Y, Wang S, Niu J. Microbial community evolution of black and stinking rivers during *in situ* remediation through micro-nano bubble and submerged resin floating bed technology. Bioresour Technol 2018;258:187–94.
[48] Liang Y, Zhao H, Deng Y, Zhou J, Li G, Sun B. Long-term oil contamination alters the molecular ecological networks of soil microbial functional genes. Front Microbiol 2016;7:60.
[49] Yuan MM, Guo X, Wu L, Zhang Y, Xiao N, Ning D, et al. Climate warming enhances microbial network complexity and stability. Nat Clim Chang 2021;11(4):343–1338.
[50] Zhou J, Deng Y, Luo F, He Z, Yang Y. Phylogenetic molecular ecological network of soil microbial communities in response to elevated CO_2. MBio 2011;2(4):e00122–e211.
[51] Wen J, Xiao Y, Song P, Sun B, Muhammad T, Ma L, et al. *Bacillus amyloliquefaciens* application to prevent biofilms in reclaimed water microirrigation systems. Irrig Drain 2021;70(1):4–15.
[52] Li L, Cao M, Yin H. Comparative roles between aragonite and calcite calcium carbonate whiskers in the hydration and strength of cement paste. Cement Concr Compos 2019;104:103350.
[53] Beech I, Cheung CS. Interactions of exopolymers produced by sulphate-reducing bacteria with metal ions. Int Biodeterior Biodegradation 1995;35(1–3):59–72.
[54] McCutcheon J, Wilson SA, Southam G. Microbially accelerated carbonate mineral precipitation as a strategy for *in situ* carbon sequestration and rehabilitation of asbestos mine sites. Environ Sci Technol 2016;50(3):1419–27.
[55] Tan SF, Raj S, Bisht G, Annadata HV, Nijhuis CA, Král P, et al. Nanoparticle interactions guided by shape-dependent hydrophobic forces. Adv Mater 2018;30(16):1707077.
[56] Yang W, Son M, Xiong B, Kumar M, Bucs S, Vrouwenvelder JS, et al. Effective biofouling control using periodic H_2O_2 cleaning with CuO modified and polypropylene dpacers. ACS Sustain Chem & Eng 2019;7(10):9582–7.
[57] Zhu J, An H, Alheshibri M, Liu L, Terpstra PMJ, Liu G, et al. Cleaning with bulk nanobubbles. Langmuir 2016;32(43):11203–11.
[58] Wu Y, Lin H, Yin W, Shao S, Lv S, Hu Y. Water quality and microbial community changes in an urban river after micro-nano bubble technology *in situ* treatment. Water 2019;11(1):66.
[59] Liu Y, Zhou Y, Wang T, Pan J, Zhou B, Muhammad T, et al. Micro-nano bubble water oxygation: synergistically improving irrigation water use efficiency, crop yield and quality. J Clean Prod 2019;222:835–43.
[60] Zhou Y, Zhou B, Xu F, Muhammad T, Li Y. Appropriate dissolved oxygen concentration and application stage of micro-nano bubble water oxygation in greenhouse crop plantation. Agric Water Manage 2019;223:105713.
[61] Huang B, Nan X, Fu C, Guo T. Study of the bubble collapse mechanism and its influencing factors on stability under ultra-low surface tension. Colloids Surf A Physicochem Eng Asp 2021;618:126440.
[62] Zhou H, Li Y, Wang Y, Zhou B, Bhattarai R. Composite fouling of drip emitters applying surface water with high sand concentration: dynamic variation and formation mechanism. Agric Water Manage 2019;215:25–43.